

Article

Cultural Heritage in the Light of Flood Hazard: The Case of the “Ancient” Olympia, Greece

Kleomenis Kalogeropoulos ^{1,*}, Konstantinos Tsanakas ², Nikolaos Stathopoulos ³, Demetrios E. Tsesmelis ⁴
and Andreas Tsatsaris ¹

¹ Department of Surveying and Geoinformatics Engineering, University of West Attica, 28 Ag. Spiridonos, 12243 Egaleo, Greece

² Department of Geography, Harokopio University of Athens, 17671 Kallithea, Greece

³ Operational Unit BEYOND-Centre of EO Research & Satellite Remote Sensing, Institute for Space Applications and Remote Sensing, National Observatory of Athens, 15236 Athens, Greece

⁴ Laboratory of Technology and Policy of Energy and Environment, School of Applied Arts and Sustainable Design, Hellenic Open University, 26335 Patras, Greece

* Correspondence: kkalogeropoulos@uniwa.gr

Abstract: Floods are natural hazards with negative environmental and socioeconomic impacts at a local and regional level. In addition to human lives, facilities, and infrastructure, flooding is a potential threat to archaeological sites, with all the implications for the cultural heritage of each country. Technological developments of recent years, particularly concerning geospatial technologies (GIS, Remote Sensing, etc.), have brought novel advantages to hydrological modelling. This study uses geoinformatics to quantify flood hazard assessment. The study area is the ungauged torrent of Kladeos River, located in Peloponnese, Greece. Geomorphological analysis combined with hydrological modelling were performed in a GIS-based environment in order to study the hydrological behavior of the Kladeos River basin. The hydrological analysis was carried out with rainfall data and hypothetical storms using a 5×5 m digital terrain model. The quantitative features of the catchment were calculated in order to determine its susceptibility to flooding. The hydro-morphometric analysis revealed stream order anomalies in the drainage network which, combined with the morphology of its upper and lower parts, enhance the possibility of flood events. The primary results indicated that there is an increased possibility of extensive flooding in the archaeological site, depending on the severity of the rainfall, since the basic geomorphological characteristics favor it. The proposed methodology calculates parameters such as flow rate, flow velocity, etc., in order to measure and quantify flood hazard and risks in the area of interest.

Keywords: flood; hazard; rainfall-runoff models; GIS; heritage



Citation: Kalogeropoulos, K.; Tsanakas, K.; Stathopoulos, N.; Tsesmelis, D.E.; Tsatsaris, A. Cultural Heritage in the Light of Flood Hazard: The Case of the “Ancient” Olympia, Greece. *Hydrology* **2023**, *10*, 61. <https://doi.org/10.3390/hydrology10030061>

Academic Editor:
Pierfranco Costabile

Received: 10 February 2023
Revised: 25 February 2023
Accepted: 28 February 2023
Published: 1 March 2023



Copyright: © 2023 by the authors. Licensee MDPI, Basel, Switzerland. This article is an open access article distributed under the terms and conditions of the Creative Commons Attribution (CC BY) license (<https://creativecommons.org/licenses/by/4.0/>).

1. Introduction

Natural disasters have a noteworthy impact in several areas worldwide, causing many deaths, damage to infrastructure and technical works, and in many cases the displacement of populations. In addition, climate change and its effects have contributed to such an extent that it is expected that in the coming years these phenomena will increase in intensity and frequency. While technological and scientific advances have made enormous strides towards dealing with them [1], the consequences are still devastating for humans, both in terms of material and household resources and in terms of loss of life. Research into these catastrophic phenomena has been on the increase in recent years [2–8]. Sustainable management of disasters and their impacts requires proper and continuous study, as well as the creation of hazard, risk, and risk maps in the man-made and natural environment [9–13].

Floods are among the most hazardous and severe natural catastrophes, affecting a significant number of people, more than 75 million [14]. In very severe floods, immediate

and proper management of their impact is essential [15–17]. In this context, flood modelling and the mapping of its results are tools that can provide solutions regarding the necessary actions and assistance to the affected areas in both the short and long term.

River flooding is a natural hazard whose consequences can potentially be very large in terms of socio-economic impact at a local and supra-regional level. 'Flood risk' refers to both the likelihood of flooding and its possible consequences for the man-made and natural environment (Directive 2007/60/EC, Chapter I, Article 2). Extreme floods resulting from heavy rainfall can cause problems for installations, technical works, and crops, resulting in the degradation of the affected areas. In addition, they can cause erosion and soil degradation which, in conjunction with forest fires, lead to further soil deterioration and gradually to desertification [18–20].

The serious consequences of the floods led the European Union (EU) to introduce measures through Directive 2007/60. Based on this EU directive, De Moel et al. [7] attempted to document the flood mapping practices followed in 29 European countries and to study the available maps and ways of using them. The conclusion was that about half of the countries had adequate maps covering the full extent of flooding, while one-third had maps covering only important areas, including Greece. Five countries were found to have very few or no flood maps [7].

Lekkas [21], lifted two basic forms of floods (downstream and upstream). Downstream are floods of long duration and high intensity in contrast to upstream floods which are of short duration and relatively low intensity [21].

In the new challenges related to the environment and natural disasters in general, sustainable water management is an important parameter for researchers and policy makers in the field of civil protection. Climate change and all the impacts it brings about, such as floods (increase in rainfall intensity and area), increase in temperature, landslides, desertification, etc., have brought human beings under a real threat, which targets them and their infrastructures. New tools are constantly being added to the scientists' quiver, concerning river hydraulics, catchment's hydrology, etc. Geospatial technologies (Geographical Information Systems, Earth Observation/Remote Sensing, etc.) are also contributing in this direction, making it easier and more straightforward to model the hydrological cycle and its individual processes [12,16,22–27].

At this stage, geospatial technologies are playing a vital role within the monitoring, modeling and predicting floods procedure. New tools and innovative techniques are used to gain a better understanding of the environment and especially its procedures such as floods [17,22,28,29].

Remote sensing data were also used in several surveys in 2007. For example, satellite data such as Landsat and SRTM DEM were combined with a rainfall-runoff model in an attempt to map flood risk in urban channels. To achieve this, Landsat 7 ETM+ images were classified (supervised classification), thus creating the land cover map, while flow and topography features were extracted by analyzing the SRTM DEM and the geographical extent of drainage axes from the topographic map of the area [12].

Pradhan [30] used logistic regression on remote sensing data through GIS to delineate potential areas at risk and generate flood susceptibility maps. The study involved potential flood areas in Malaysia and the objective was to present them in a susceptibility map produced through statistical modelling in a GIS environment. The methodology aimed to create a geographical database containing all the necessary spatial data (topographic, geological, land cover, hydrological, DEM, GPS and rainfall data), which was later processed to calculate the calibration of each factor using logistic regression. The flood susceptibility layer was synthesized by superimposing the generated layers (factors). An interesting coupling, in terms of flood modelling, was made by Ranaee et al. [31], who simulate flooding channels using commercial and non-commercial software (HEC-HMS and MIKE11). Chen et al. [32] used EO and GIS in spatial hydrological analysis. Finally, as part of the evolution of older methods, Du et al. [33] proposed a new spatially distributed direct hydrograph varying in time (used in this work) incorporating SCS curve number [34,35],

which was analogous to the model of Melesse and Graham [27]. Additionally, in a study, a new tool for flood hazard mapping provided, emerging an procedure for flood hazard mapping in presence of numerous gauging stations, based on the use of high resolution LiDAR resulting digital topography and intermittent hydrometric data recorded by various monitoring stations [36]. In absence of hydrometric data the use of SCS number method for mapping flood areas can be useful [37], whilst hydrographs can also be derived via statistics approaches [38].

With regard to Greece, there is a long history of flooding, escorted by a significant quantity of deaths. Many catchments in the country are formed by streams whose central bed has a branching shape. They are small in area and characterized by steep morphological gradients. These river systems are intermittent and have no water during most of the year. However, during extreme rainfall events their flow can reach extremely high values and become very active, causing extreme flash floods of low frequency but high intensity [39]. Several areas in Greece, including coastal towns built on estuaries, suffer the harmful consequences of dangerous extreme floods [40]. Their negative consequences are maximized in built-up riparian places as forestalling is a parameter that is frequently overlooked by both planners and the state when implementing urban development plans [10,41,42]. Despite the multiple negative effects of flash floods on small ephemeral rivers, their hydrological study and monitoring in the country has always been difficult, mainly due to the lack of a dense network of rainfall and river flow measuring stations [43,44]. Protection of monuments, buildings and archaeological sites against natural disasters are critical for a sustainable cultural heritage [45,46], while the damage from disasters such as floods can be irreversible [47].

This research study analyses the hydrological and geomorphological regime of Kladeos River Basin and attempts to quantify and assess the possible flooding threat of the archeological site of Ancient Olympia, which is located very close to the basin's outlet. The methodology, developed in a GIS, challenges to study the natural procedures of a real and hypothetical rainfall incident (358 mm of rainfall) in the Kladeos River, Peloponnese. For this purpose, a rainfall-runoff model is used to calculate the spatially distributed synthetic unit hydrograph. The basin response was very fast in both cases. In fact, the simulation of the actual event showed that the water travel time was shorter than the travel time of the hypothetical event, although the hypothetical event was more severe. The results highlighted the augmented possibility of flooding in the archeological site in case of similar, to the ones modelled, or even more intense rainfall events.

2. Study Area

The Kladeos River, a river god in Greek mythology [48] is an intermittent stream located in the western part of the Peloponnese (as shown in Figure 1). It originates from the foothills of Mount Foloe, flows to the northwest, and at its lower reaches, takes a sharp turn to the south before merging with the Alpheios River. The Kladeos catchment area covers a total of 33.23 km², reaching a height of 618 m. The basin extends along a southwest-northeast axis and has an asymmetrical shape, with the main channel occupying mostly the southern part of the catchment. The drainage basin consists mostly of post-Alpine Plio-Quaternary formations, including marls, sands, sandstones, and conglomerates, with limited alluvial deposits found in the channels of the lower reaches of the drainage network. The region has a typical Mediterranean climate, classified as Csa under the Köppen climate classification system [49,50], with hot and dry summers and mild and wet winters.

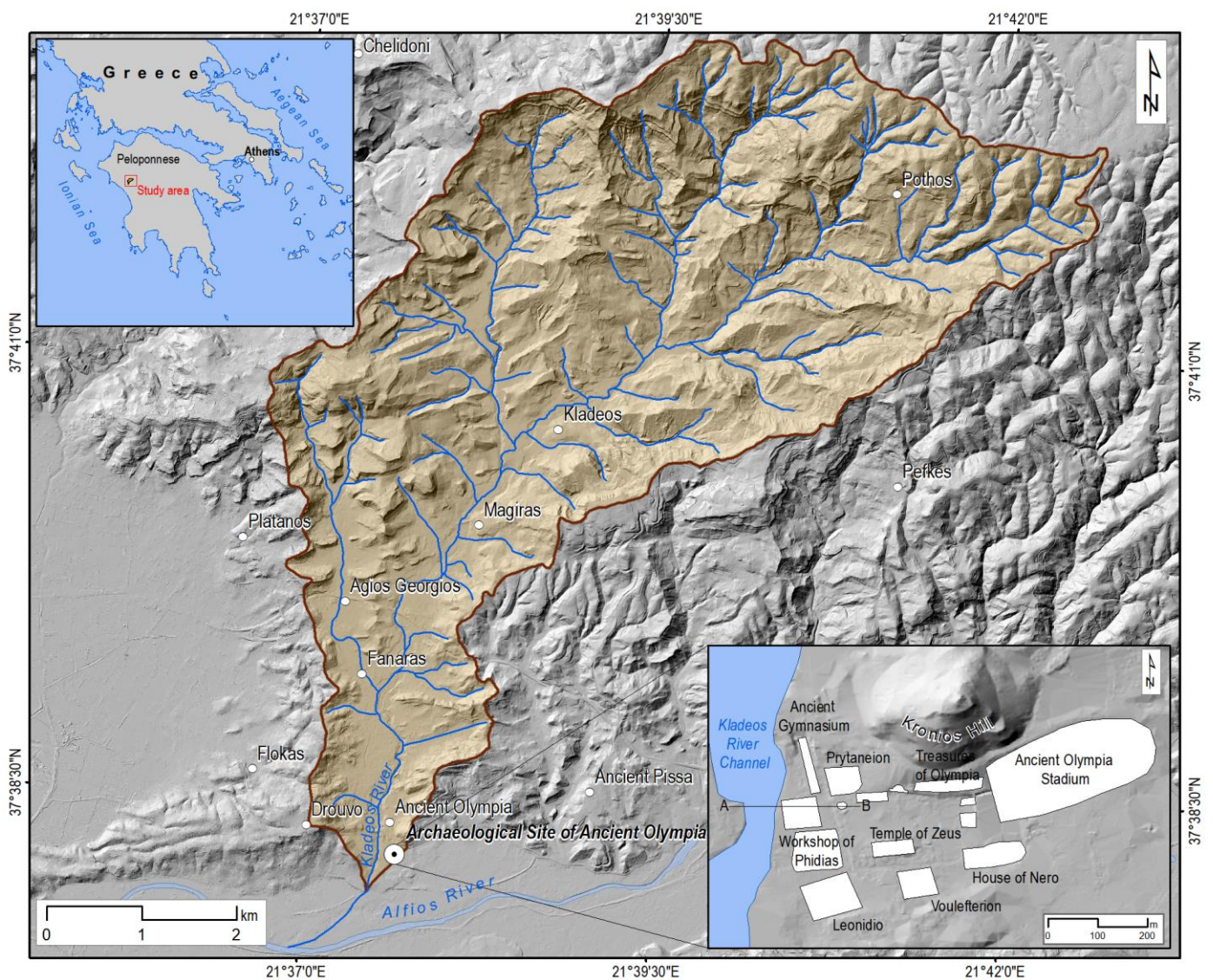


Figure 1. Location of Kladeos River drainage basin in NW Peloponnese, Greece (A-B is the Cross section at the lower reaches of the main channel depicted in Figure 6a).

One of the unique features of the area is that the Kladeos River flows through the city of Ancient Olympia (with a population of 835 inhabitants) and near the archaeological site of Ancient Olympia, which attracts over 500,000 visitors each year. The Kladeos River is a contributor of the Alpheios River. Both rivers are known for “providing” floods since ancient times (fourth century AD) [51] and modern times [52].

The archaeological site (Figure 2) is located less than 50 m away, and almost 1.5 m higher than the Kladeos channel in its lower reaches.



Figure 2. The archaeological site of ancient Olympia (Source: Google Earth).

3. Methodology

3.1. Hydrological and Morphometric Analysis

The correlation of the topography to the hydrological/geomorphological features demands the calculation of the hydromorphometric characteristics of the river. The hydrological network and the individual catchments were automatically derived from a 5 m cell size Digital Elevation Model, and classified according to the Strahler system [53]. Furthermore, the bifurcation ratios and the hierarchical drainage by stream order were calculated to examine the anomalies in the development of the network [54]. Moreover, a geomorphological map of the drainage basin was produced to detect the foremost geomorphological features inside the drainage basin and to investigate the natural causes of past flood events [55]. For this purpose, a Red Relief Image Map (R.R.I.M) was produced in QGIS software. This method is based on multi-layered topographic information computed from three-dimensional (DEM). The basic concept is the multiplication of three element layers, topo-graphic slope, positive and negative openness. Red Relief Image Maps can visualize not only topographic slopes, but also concavities and convexities at the same time. This method was proved ideal for the recognition and mapping of landforms within the Kladeos River catchment which were also validated by fieldwork observations. Furthermore, a longitudinal profile and a cross section were constructed in order to investigate the variations in morphological slopes along the main channel as well as at its lower reaches in the vicinity of the archaeological site of Olympia.

3.2. Hydrological Model Development

3.2.1. Hypothetical and Real Scenario Analysis

Flood hazard was assessed by simulating the rainfall of two main scenarios. The first is a real event and the second is a hypothetical one. The real flood event occurred on 5 February 2012. The catastrophic flood was caused by extreme rainfall (151.4 mm was recorded in 9 h at the weather stations closest to the flooded area). The flood height

reached 358 mm in 43 h and caused extensive damage to public infrastructure and private properties.

The hypothetical event was selected to assess the possible flood hazard from a rainfall of this magnitude and intensity on the Kladeos River. The characteristics of this scenario were the same to the real one but rainfall is distributed differently within the same time period.

3.2.2. Entry Data

The procedure was carried out within a GIS context. Therefore, a digital spatial database was planned, which consists of the following layers:

1. Digital Elevation Model (DEM). A key aspect of the proposed process is the need to create a hydrologically valid DEM while preserving the actual morphological features of the study area. This makes the pre-processing of the DEM and its derivatives necessary and essential. A 5×5 m DEM was used (Greek Cadaster).
2. Manning's coefficient of roughness. For the purposes of the simulation, this coefficient was derived from a land cover map (Ilot Project, Greece). The resulting categorization according to land cover and the correspondence between each category and the Manning roughness coefficient is shown in the following table (Table 1).

Table 1. Land cover and roughness coefficient by Manning (Ilot, Greece, [4]).

Description	Manning's Roughness Coefficient
Forest areas	0.2
Urban area	0.015
Grassland-Pasture land	0.1
Arable crops	0.1
Permanent crops	0.1
Olive grove	0.15
Vineyard	0.05
Mixed forest land	0.2
Urban mixed areas	0.015
Meadows and grassland mixed	0.1
Edible mixed	0.1
Permanent mixed	0.1
Mixed olive groves	0.15
Mixed vineyard	0.05

3.2.3. Hydrological Modeling

The main objective of each simulation is to estimate the maximum flow, resulting from a precipitation incident. The methodological flowchart is shown in Figure 3.

The hydrograph intercepts of runoff over this common duration (flood base time) are proportional to rainfall (amount) [34]. To apply unit hydrograph, the observed hydrographs of the catchment are required. That is, hydrographs from rainfall and flow measurements during specific events.

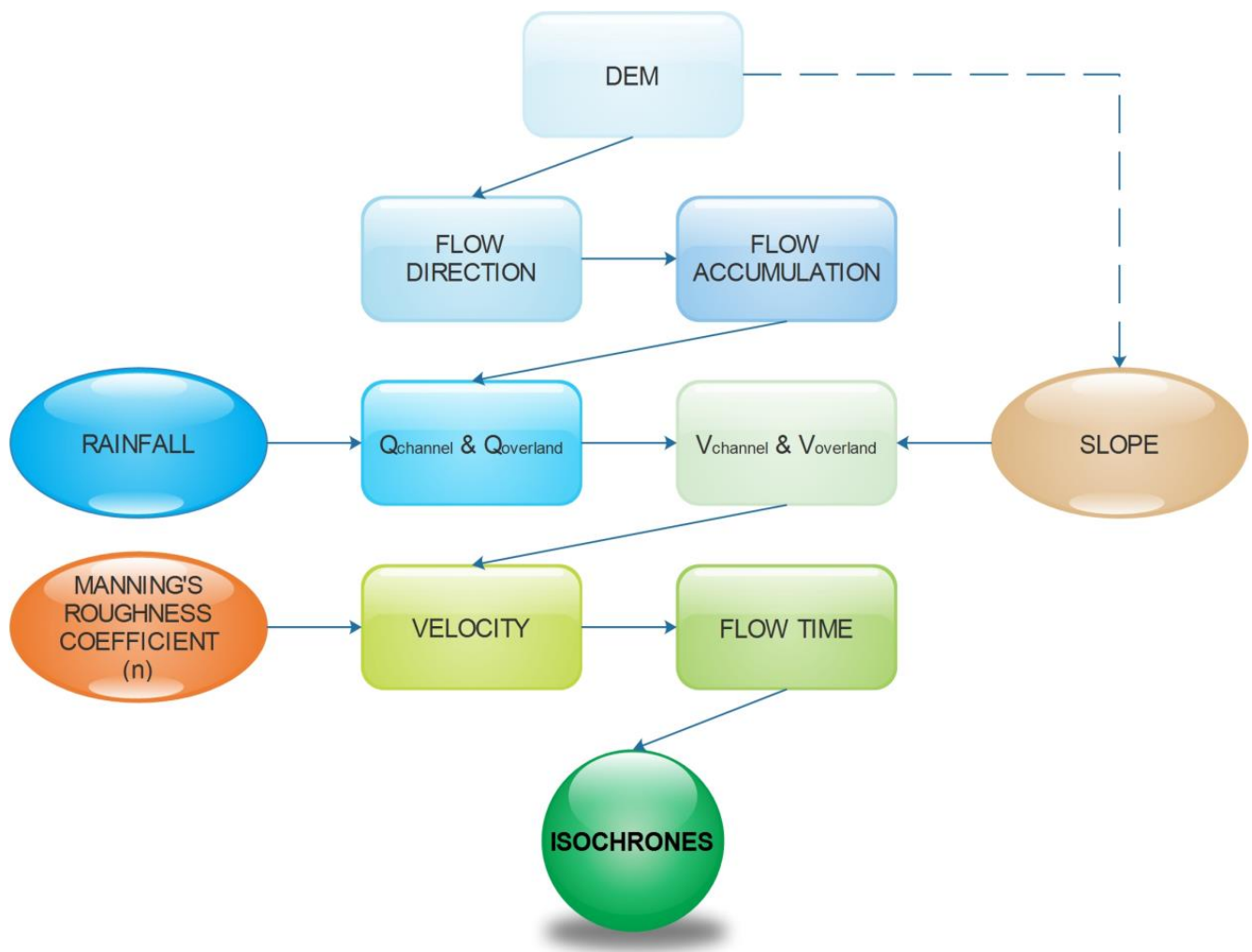


Figure 3. The flow chart of the methodology ($Q_{channel}$, $Q_{overland}$, $V_{channel}$ and $V_{overland}$ are the discharge within the channel, the overland discharge, the velocity within the channel and the overland velocity of the water, respectively).

Their construction also requires the existence of data from real events in basins adjacent to or with similar characteristics to that of the study area. It is a given, however, that in this case the predictive value of the model contains greater uncertainty [43]. To separate the stratified flow from the flow concentrated in the beds of the hydrographic network, a threshold of interstitial cells (or equivalent drainage area) was defined. This separated these two types of flow and at the same time defined the hydrographic network. In this application, the threshold was taken equal to 100 cells. Having extracted the accumulated flow level and rainfall levels, the flow in the hydrographic network was calculated based on the reclassified level of accumulated flow. The discharge in the network branches ($Q_{channel}$ in m^3/s) was calculated from the following formula:

$$Q_{channel} = i_e \times Flow\ accumulation \times cell.size^2 \quad (1)$$

where i_e is the intensity of the rain (in m/s).

Then, overland discharge ($Q_{overland}$ in m^3/s) was calculated. The upstream flow was derived from the flow direction plane and the equation was applied:

$$Q_{overland} = i_e \times l_{upstream} \quad (2)$$

where i_e is again the rainfall intensity (in m/s) and $l_{upstream}$ (in m) is the length of the upstream runoff.

To calculate the runoff time, the flow velocity is required. The flow velocity on the watershed slopes ($V_{overland}$ in m/s) was estimated for each individual cell using the following formula derived by combining Manning's formula for uniform steady flow and the continuity equation [33].

$$V_{overland} = \frac{Q_{overland}^{0.4} \times S_0^{0.3}}{n^{0.6}} \quad (3)$$

where S_0 is the cell slope (dimensionless) and n is the Manning's roughness coefficient (in $s/m^{1/3}$).

The flow velocity in the beds of the hydrographic network ($V_{channel}$ in m/s) was calculated according to the following equation obtained by combining Manning's formula with the continuity equation [33]:

$$V_{channel} = \frac{Q_{channel}^{0.25} \times S_0^{0.3}}{n^{0.75}} \quad (4)$$

After estimating the flow velocity for each cell of the Kladeos stream catchment following the above procedure, the time required for water to cross each cell was calculated and reclassified in order to obtain the isochronous curves.

4. Results and Discussion

4.1. Hydro-Morphometric Analysis

The classification of the drainage network according to Strahler [53], as well as the bifurcation ratios and the % divergence between actual and ideal number of streams per order are presented in Table 2. The quantitative analysis showed high values of negative divergence (−13.63% to −40%) between the actual and ideal number of streams of 1st, 2nd, 3rd and 4th order. This means that the drainage network is poorly developed and this could be attributed to the tectonic activity as the Kladeos basin is developed in the eastern part of the tectonically and seismically active basin of Pyrgos–Olympia, which is the main neotectonic structure of the study area.

Table 2. Hydromorphological relations for the Kladeos River catchment.

Stream Order (u)	Number of Streams (Nu)	Bifurcation Ratio (R_b)	Mean Bifurcation Ratio ($R_{b(mean)}$)	Ideal Stream Number	Divergence (%)	Total Drainage Basin Area (km^2)
1	95	$R_{b1,2} = 4.13$		110	−13.63	17.67
2	23	$R_{b2,3} = 3.83$		34	−32.35	14.55
3	6	$R_{b3,4} = 3.0$	3.24	10	−40	16.62
4	2	$R_{b4,5} = 2.0$		3	−33.33	14.32
5	1			1	0	33.23

The analysis of the hierarchical drainage by stream order showed major anomalies regarding the 1st, 2nd and 3rd order streams (Table 3 and Figure 4).

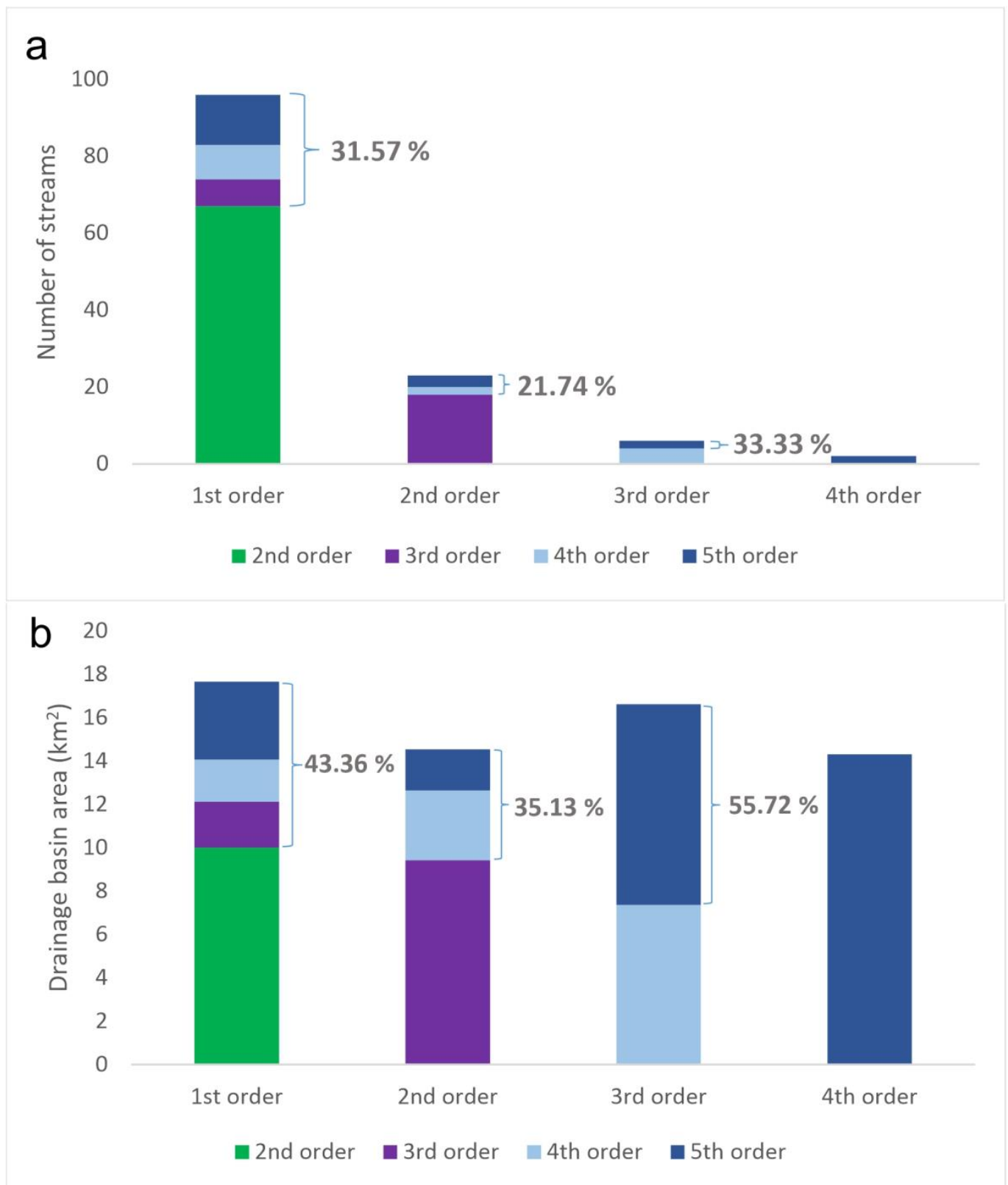


Figure 4. Hierarchical drainage by stream order for Kladeos River drainage network (a. Number of streams and b. Drainage basin area).

Table 3. Hierarchical drainage for the Kladeos drainage network.

Drainage by Stream Order	Number of Streams		% of Total Number by Order		Drainage Basin Area (km ²)		% of Total Area by Order	
1st to 2nd	65		68.43		10.01		56.64	
1st to 3rd	8	} 30	8.42	} 31.57	2.12	} 7.66	11.99	} 43.36
1st to 4th	9		9.47		1.94		10.97	
1st to 5th	13		13.68		3.60		20.40	
2nd to 3rd	18		78.26		9.44		64.87	
2nd to 4th	2	} 5	8.69	} 21.74	3.20	} 5.11	22.0	} 35.13
2nd to 5th	3		13.05		1.91		13.13	
3rd to 4th	4		66.67		7.36		44.28	
3rd to 5th	2		33.33		9.26		55.72	
4th to 5th	2		100		14.32		100	

In particular, 31.57% of the 1st order streams bypass the 2nd order and flow into the 3rd, 4th, or 5th order streams. The drainage basins for these streams cover an area of 7.66 km², which is approximately 23% of the total basin area. Additionally, 13.68% of the 1st order streams flow directly into the main channel, causing an increased discharge and heightening the risk of flooding in the lower reaches. On the other hand, 21.74% of the 2nd order streams flow into the 4th or 5th order streams, with their drainage basins accounting for 35.13% of the total area of 2nd order streams. Meanwhile, 55.72% of the 3rd order streams drain directly into the main channel, corresponding to 27.8% of the total drainage basin area (5th order). Therefore, in the case of extreme rainfall, nearly a third of the total drainage basin flows directly into the main channel of Kladeos, which amplifies the catchment's quick response to heavy rainfall.

The geomorphological mapping of the Kladeos River drainage basin is presented in Figure 5. The geometry of the basin is elongated and asymmetric since the main channel occupies mainly the southern part of the basin. This asymmetry could be attributed to the high erodibility of the silt, sand and gravel formations which occupy the southern part of the basin as opposed to the less erodible conglomerates which occupy the northern part.

The largest part of the drainage basin, especially the lower reaches is characterized by a gentle relief while the upper reaches at the NE part of the basin is dominated by steep slopes and relatively sharp ridge crests between the streams. The deposition of sediments at the lower reaches of the drainage network (probably linked with past flood events) and their consequent incision, lead to the formation of quite extensive fluvial terraces within the channels. An alluvial cone has formed at the junction of the Kladeos torrent and the Alpheios River, as a result of the accumulation of sediments from the Kladeos drainage basin deposited by the river.

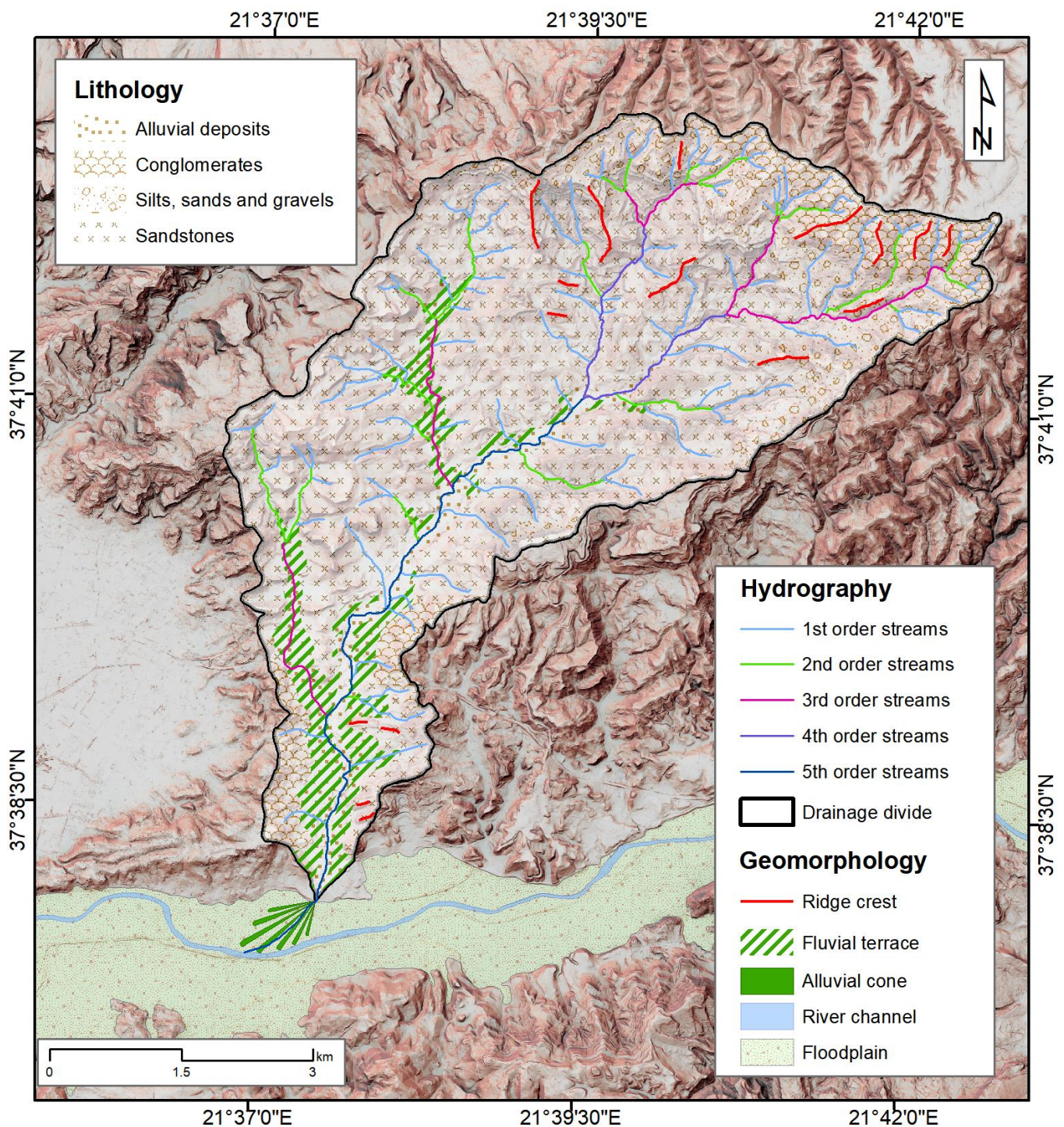


Figure 5. Simplified geomorphological map of the Kladeos River drainage basin.

The longitudinal profile of the Kladeos River's main channel, as displayed in Figure 6a, reveals a topographic landscape that transitions from a mountainous terrain in the northeast part of the basin to relatively flat lowlands near the lower reaches of the river. In the mountainous region, the slopes are quite steep, reaching a gradient of 16.5%, while in the low-lying areas, the gradient is much gentler at 1.36%. It is noteworthy that the steep portions of the drainage network, correspond to the 3rd order streams that anomalously drain directly into the main channel. The combination of these two factors leads to a substantial increase in water volume and velocity that flows into low gradient areas, thereby enhancing the likelihood of a flood event.

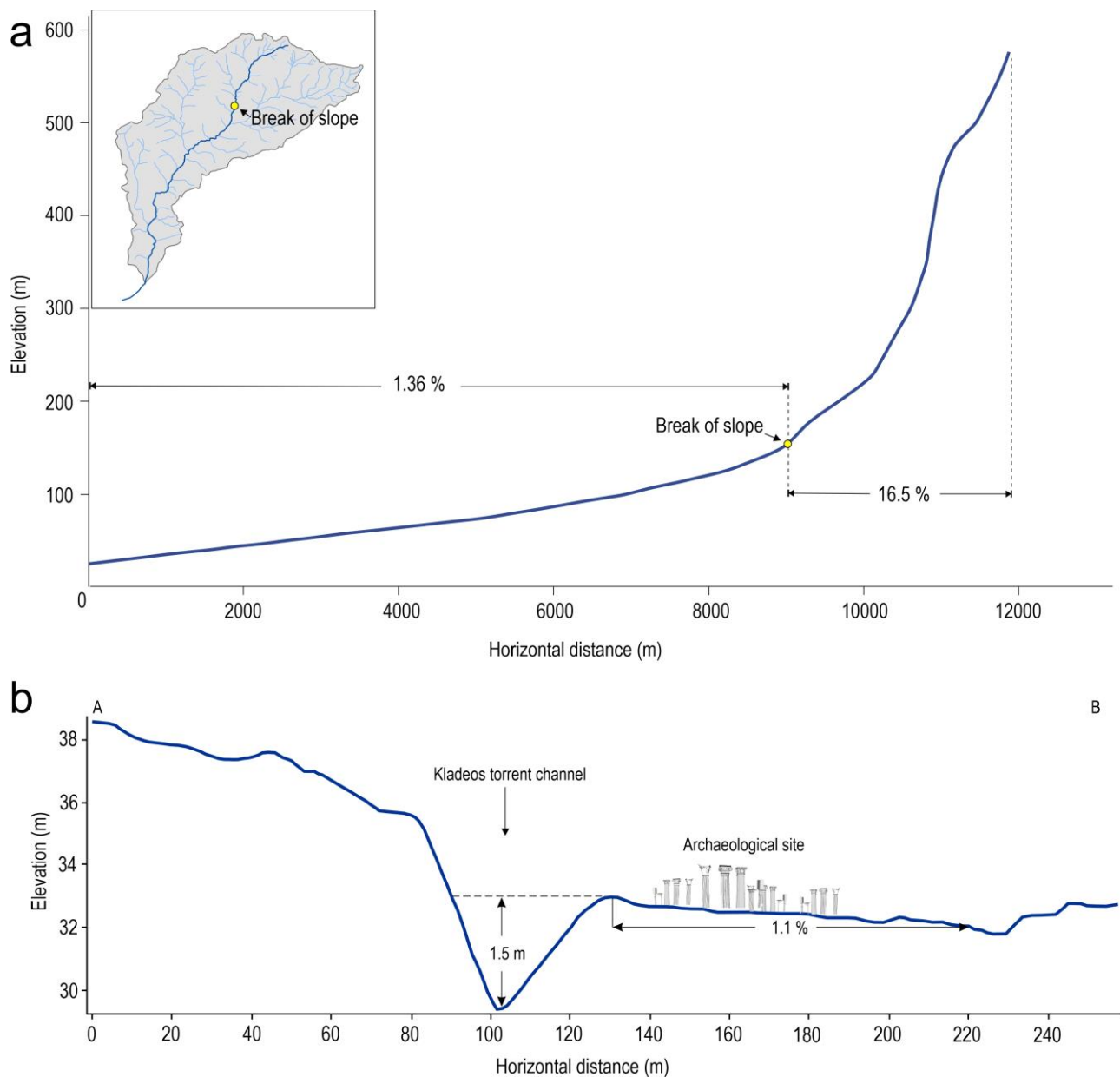


Figure 6. (a) Longitudinal profile along the main channel of the Kladeos River. (b) Cross section at the lower reaches of the main channel. The location of the cross section is depicted in Figure 1.

Additionally, the cross-section of the lower reaches of the Kladeos River's main channel, as depicted in Figure 6b, reveals that the archaeological site of Ancient Olympia is located in close proximity to the river, with a distance of less than 20 m from the eastern bank. The site rests on a relatively flat surface that slopes down towards the east at a gradient of 1.1%. At the eastern edge of this surface, roughly 100 m east of the Kladeos channel, there is a sudden break in the slope that impedes the flow of water in the event of a flood. Furthermore, the low depth of the Kladeos channel at this point, approximately 1.5 m, and the asymmetry of the channel cross-section caused by the presence of less erodible conglomerates on the western flank, make the archaeological site of Olympia the only place for water to flow into during a flood event. As a result, the unique combination of the area's landscape morphology and the hydro-morphometric characteristics of the upper part of the basin leads to the rapid accumulation of a large volume of water that the main channel is unable to effectively accommodate.

4.2. Hydrological Modelling

The hydrological model, which was utilized for the simulation of the surface runoff within the Kladeos River basin, relied on the creation of a layer that depicts isochronous curves within the basin.

The isochronous curves map shows that the runoff times for points corresponding to the beds of the branches of the hydrographic network are shorter than the times for points in the basin corresponding to slopes where water discharges surface runoff as sheet flow. From the reclassified level of isochronous surfaces, based on the number of cells of each class, its extent can be deduced. For the construction of the hydrograph, the time pulse was considered as a time interval of 1 h. Thus, the amount of rainfall received per hour by each class of isochronous surfaces was calculated and in this way the flow was estimated, resulting the synthetic unit direct hydrograph that depicts the variation of the flow per hour at the outlet of the stream basin [43].

Several simulations were carried out, changing the precipitation distribution in order to evaluate two different models, the final hypothetical and the real one. The next figure shows the two main versions of the hypothetical and the real scenario (Figure 7).

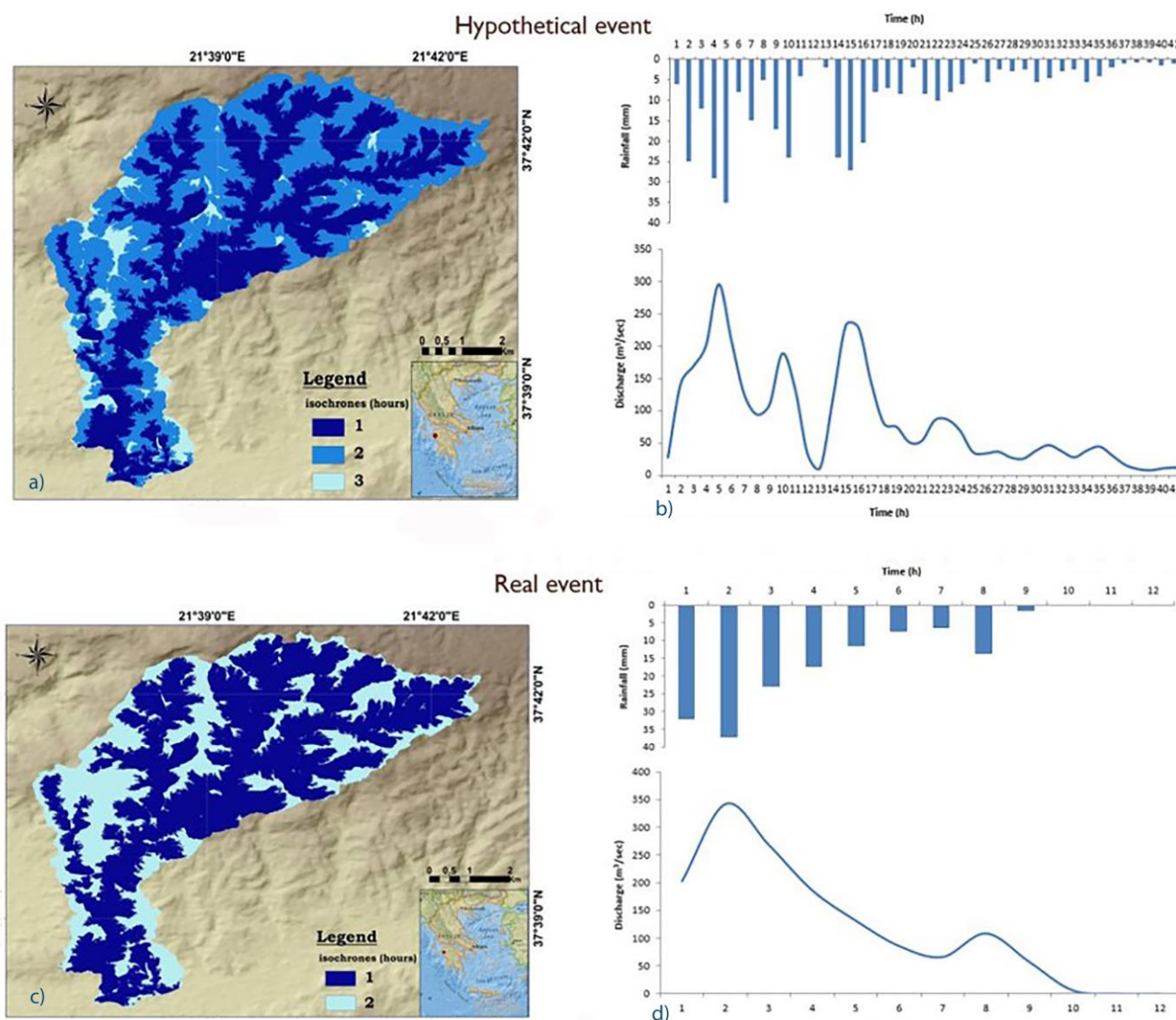


Figure 7. The hypothetical event and its results: ((a) isochrones map, (b) rainfall-discharge chart) and the real event hydrological results ((c) isochrones map, (d) rainfall-discharge chart).

The form of the produced hydrograph of the real event is characteristic of a flash flood. Both graphs show the basin response to heavy rainfall, which is immediate and very fast.

The hypothetical event is characterized by three main vertices:

- First peak: 265.61 m³/s at the 5th h (t critical)
- Second peak: 188.06 m³/s at the 10th h.
- Third peak: 231.67 m³/s at the 15th h.

The actual event is characterized by two main peaks:

- First peak: 341.48 m³/s at the 2nd h (t critical)
- Second peak: 108.54 m³/s at the 8th h.

The critical result is the fact that in the real event the basin response is faster (2 h isochrones) compared to the hypothetical event where the response is slower (3 h isochrones).

In conclusion, the basin's response was very fast in both cases. The simulations showed that the water travel time was shorter in the actual event than the travel time of the hypothetical event, although the hypothetical event was more severe. This is in line with the results of Fountoulis and Mavroulis [56], who simulated river flow in Kladeos and the instantaneous unitary hydrograph had a form which was interpreted that within the Kladeos catchment, there are places that they discharge simultaneously in a severe flood, causing a lot of problems.

Finally, there are two main limitations in the present analysis. The first one concerns the spatial resolution of the DEM (5 × 5 m pixel size). Although, it is an adequate resolution compared to the basin's extent and considering the fact that the produced results (based on this scale analysis) exhibit a very good understanding of the characteristics and response of the basin, an even more-detailed DEM would offer a more accurate analysis of the basin's response to the two rainfall scenarios that were tested. Furthermore, another noteworthy limitation is the lack of field measurements, so that the results of this analysis can be compared and assessed with in situ data. The possible existence of water discharge measurements (in various places in the basin), in terms of volume and time reaching the basin's outlet, would help validate and/or improve/adjust the theoretical steps followed in this analysis. More importantly, ground-truth data close to the archeological site would offer important information for calibrating the algorithmic model and refining the theoretical assessment on the site's flood hazard.

5. Conclusions

The likelihood of a flash flood event in Kladeos River can be influenced by various factors related to the drainage network and its hydromorphological characteristics. These include high values of negative divergence, where the actual number of streams deviates from the ideal number of streams in 1st, 2nd, 3rd, and 4th order by up to 40%, as well as irregularities in the stream order, with 31.57% of 1st order streams bypassing the 2nd order and flowing into 3rd, 4th, or 5th order streams. Additionally, 35.13% of 2nd order drainage basins drain directly into 4th and 5th order streams, and 55.72% of the 3rd order catchment area drains directly into the main channel, contributing to high water discharge during extreme rainfall events. Moreover, the drainage network's landscape morphology exacerbates the potential for flash floods. The steep slopes in the upper part of the basin (3rd order streams) combined with the low gradients along the lower reaches of the main channel result in high flow velocities of large water volumes that can overburden the main channel. The proximity of the archaeological site of Ancient Olympia to the Kladeos main channel, and its location on a flat surface with a low gradient that dips to the east, further increases the risk of flooding. The abrupt break of slope on the eastern side of the site, the low channel depth, and the channel asymmetry due to the less erodible conglomerates on the western flank, can cause water to accumulate rapidly in the case of extreme rainfall events, leading to a significant flood risk.

The analysis presented in this work highlighted the fact that the archeological site of Ancient Olympia is at immediate risk, in the case of a similar rainfall event (to the modelled ones). Moreover, considering the predicted trends due to climate change, even more extreme rainfall events, in intensity and frequency, are expected, constituting the possibility of flood occurrence in the archeological site almost a certainty, if no appropriate measures are adopted. In any other case, severe flood events may have significant cultural and socio-economic impacts both at a regional and national level.

From a scientific and technological point of view, the synthetic UH form, a result of the model used, for the exit of the basin can, under conditions, be used in a number of cases for the study of similar phenomena. In every hydrograph there are two values of vital importance. These are the maximum discharge and the critical time between maximum rainfall and maximum discharge. These two quantities can be used in the study of technical works and infrastructures, such as bridges over rivers, in road construction, etc. They are also critical quantities in order to create reports on the risk of flooding, overall risk in an area, in flood forecasting, etc. It is used by the hydraulic engineers, in addition, in the study of rivers, arrangement of streams when there is a lack of data (meteorological, hydrometric, etc.).

It is therefore understandable that these kind of hydrological models can become tools for policy makers and decision makers. It is also understood that Geospatial Technologies such as Geographical Information Systems, Earth Observation/Remote Sensing, etc., can play a decisive role in decision-making related to the effective response to natural disasters and ultimately to the sustainable management of the environment.

Author Contributions: Conceptualization, K.K.; methodology, K.K., A.T., N.S., D.E.T. and K.T.; validation, K.K.; writing—original draft preparation, K.K., A.T., N.S., D.E.T. and K.T.; validation, K.K.; K.T., N.S.; writing—review and editing, K.K., A.T., N.S., D.E.T. and K.T.; validation, K.K.; visualization, K.K.; supervision, K.K.; All authors have read and agreed to the published version of the manuscript.

Funding: This research received no external funding.

Data Availability Statement: Not applicable.

Conflicts of Interest: The authors declare no conflict of interest.

References

1. Kalogeropoulos, K.; Tsatsaris, A.; Stathopoulos, N.; Tsesmelis, D.E.; Psarogiannis, A.; Pissias, E. GIS & Remote Sensing for Local Development. Reservoirs Positioning. In *GeoInformatics for Geosciences Advanced Geospatial Analysis Using RS, GIS & Soft Computing*; Stathopoulos, N., Tsatsaris, A., Kalogeropoulos, K., Eds.; Earth Observation; Elsevier: Amsterdam, The Netherlands, 2023; ISBN 978-0-323-98983-1. (In press)
2. Smith, K.; Petley, D.N. *Environmental Hazards: Assessing Risk and Reducing Disaster*, 5th ed.; Routledge: Abingdon, UK, 2009.
3. Kalogeropoulos, K.; Stathopoulos, N.; Psarogiannis, A.; Pissias, E.; Louka, P.; Petropoulos, G.P.; Chalkias, C. An Integrated GIS-Hydro Modeling Methodology for Surface Runoff Exploitation via Small-Scale Reservoirs. *Water* **2020**, *12*, 3182. [[CrossRef](#)]
4. Kalogeropoulos, K.; Chalkias, C. Modelling the Impacts of Climate Change on Surface Runoff in Small Mediterranean Catchments: Empirical Evidence from Greece. *Water Environ. J.* **2013**, *27*, 505–513. [[CrossRef](#)]
5. Dinh, Q.; Balica, S.; Popescu, I.; Jonoski, A. Climate Change Impact on Flood Hazard, Vulnerability and Risk of the Long Xuyen Quadrangle in the Mekong Delta. *Int. J. River Basin Manag.* **2012**, *10*, 103–120. [[CrossRef](#)]
6. Glas, H.; Rocabado, I.; Huysentruyt, S.; Maroy, E.; Salazar Cortez, D.; Coorevits, K.; De Maeyer, P.; Deruyter, G. Flood Risk Mapping Worldwide: A Flexible Methodology and Toolbox. *Water* **2019**, *11*, 2371. [[CrossRef](#)]
7. de Moel, H.; van Alphen, J.; Aerts, J.C.J.H. Flood Maps in Europe—Methods, Availability and Use. *Nat. Hazards Earth Syst. Sci.* **2009**, *9*, 289–301. [[CrossRef](#)]
8. Norman, L.M.; Huth, H.; Levick, L.; Shea Burns, I.; Phillip Guertin, D.; Lara-Valencia, F.; Semmens, D. Flood Hazard Awareness and Hydrologic Modelling at Ambos Nogales, United States-Mexico Border: Flood Hazard Awareness and Hydrologic Modelling at Ambos Nogales. *J. Flood Risk Manag.* **2010**, *3*, 151–165. [[CrossRef](#)]
9. Maantay, J.; Maroko, A. Mapping Urban Risk: Flood Hazards, Race, & Environmental Justice in New York. *Appl. Geogr.* **2009**, *29*, 111–124. [[CrossRef](#)]
10. Stamellou, E.; Kalogeropoulos, K.; Stathopoulos, N.; Tsesmelis, D.E.; Louka, P.; Apostolidis, V.; Tsatsaris, A. A GIS-Cellular Automata-Based Model for Coupling Urban Sprawl and Flood Susceptibility Assessment. *Hydrology* **2021**, *8*, 159. [[CrossRef](#)]

11. Smith, K. *Environmental Hazards: Assessing Risk and Reducing Disaster*, 6th ed.; Routledge Taylor & Francis Group: London, UK; New York, NY, USA, 2013; ISBN 978-0-415-68105-6.
12. Tapia-Silva, F.O.; Nuñez, J.M.; López-López, D. Using SRTM DEM, Landsat ETM+ Images and a Distributed Rainfall-runoff Model to Define Inundation Hazard Maps on Urban Canyons. In Proceedings of the 32nd International Symposium on Remote Sensing of Environment, San Jose, Costa Rica, 25 June 2007.
13. Alaghmand, S.; Abdullah, R.B.; Abustan, I.; Vosough, B. GIS-Based River Flood Hazard Mapping in Urban Area (a Case Study in Kayu Ara River Basin, Malaysia). *Int. J. Eng. Technol.* **2010**, *2*, 488–500.
14. Hewitt, K. *Regions of Risk*; Routledge: Abingdon, UK, 2014; ISBN 978-1-317-89417-9.
15. Wang, Y. Using Landsat 7 TM Data Acquired Days after a Flood Event to Delineate the Maximum Flood Extent on a Coastal Floodplain. *Int. J. Remote Sens.* **2004**, *25*, 959–974. [[CrossRef](#)]
16. Gioti, E.; Riga, C.; Kalogeropoulos, K.; Chalkias, C. A GIS-Based Flash Flood Runoff Model Using High Resolution DEM and Meteorological Data. *EARSeL eProc.* **2013**, *12*, 33–43.
17. Kalogeropoulos, K.; Karalis, S.; Karymbalis, E.; Chalkias, C.; Chalkias, G.; Katsafados, P. Modeling Flash Floods in Vouraikos River Mouth, Greece. In Proceedings of the 10th Global Congress on ICM: Lessons Learned to Address New Challenges, EMECS 2013—MEDCOAST 2013 Joint Conference, Marmaris, Turkey, 30 October–3 November 2013; Volume 2, pp. 1135–1146.
18. Tsesmelis, D.E. Development, Implementation and Evaluation of Drought and Desertification Risk Indicators for the Integrated Management of Water Resources. Ph.D. Dissertation, Department of Natural Resources Management & Agricultural Engineering, Agricultural University of Athens, Athens, Greece, 2017.
19. Tsesmelis, D.E.; Karavitis, C.A.; Kalogeropoulos, K.; Zervas, E.; Vasilakou, C.G.; Skondras, N.A.; Oikonomou, P.D.; Stathopoulos, N.; Alexandris, S.G.; Tsatsaris, A.; et al. Evaluating the Degradation of Natural Resources in the Mediterranean Environment Using the Water and Land Resources Degradation Index, the Case of Crete Island. *Atmosphere* **2022**, *13*, 135. [[CrossRef](#)]
20. Tsesmelis, D.E.; Vasilakou, C.G.; Kalogeropoulos, K.; Stathopoulos, N.; Alexandris, S.G.; Zervas, E.; Oikonomou, P.D.; Karavitis, C.A. Drought Assessment Using the Standardized Precipitation Index (SPI) in GIS Environment in Greece. In *Computers in Earth and Environmental Sciences*; Elsevier: Amsterdam, The Netherlands, 2022; pp. 619–633. ISBN 978-0-323-89861-4.
21. Lekkas, E. Natural & Technological Disasters; Access Pre-Press. 2000. Available online: https://www.researchgate.net/publication/226053524_Natural_and_Technological_Disasters (accessed on 24 February 2023).
22. Stathopoulos, N.; Kalogeropoulos, K.; Polykretis, C.; Skrimizeas, P.; Louka, P.; Karymbalis, E.; Chalkias, C. Introducing Flood Susceptibility Index Using Remote-Sensing Data and Geographic Information Systems. In *Remote Sensing of Hydrometeorological Hazards*; Earth Sciences, Engineering & Technology, Geography; CRC Press: Boca Raton, FL, USA, 2017; ISBN 978-1-315-15494-7.
23. Liu, Y.B.; Gebremeskel, S.; De Smedt, F.; Hoffmann, L.; Pfister, L. A Diffusive Transport Approach for Flow Routing in GIS-Based Flood Modeling. *J. Hydrol.* **2003**, *283*, 91–106. [[CrossRef](#)]
24. Nikolaos, S.; Kleomenis, K.; Elias, D.; Panagiotis, S.; Panagiota, L.; Vagelis, P.; Christos, C. A Robust Remote Sensing–Spatial Modeling–Remote Sensing (R-M-R) Approach for Flood Hazard Assessment. In *Spatial Modeling in GIS and R for Earth and Environmental Sciences*; Elsevier: Amsterdam, The Netherlands, 2019; pp. 391–410. ISBN 978-0-12-815226-3.
25. Gigović, L.; Pamučar, D.; Bajić, Z.; Drobnjak, S. Application of GIS-Interval Rough AHP Methodology for Flood Hazard Mapping in Urban Areas. *Water* **2017**, *9*, 360. [[CrossRef](#)]
26. Kourgialas, N.N.; Karatzas, G.P. Flood Management and a GIS Modelling Method to Assess Flood-Hazard Areas—A Case Study. *Hydrol. Sci. J.* **2011**, *56*, 212–225. [[CrossRef](#)]
27. Mesle, A.M.; Graham, W.D. Storm Runoff Prediction Based on a Spatially Distributed Travel Time Method Utilizing Remote Sensing and GIS. *J. Am. Water Resour. Assoc.* **2004**, *40*, 863–879. [[CrossRef](#)]
28. Tsanakas, K.; Gaki-Papanastassiou, K.; Kalogeropoulos, K.; Chalkias, C.; Katsafados, P.; Karymbalis, E. Investigation of Flash Flood Natural Causes of Xirolaki Torrent, Northern Greece Based on GIS Modeling and Geomorphological Analysis. *Nat. Hazards* **2016**, *84*, 1015–1033. [[CrossRef](#)]
29. Tsatsaris, A.; Kalogeropoulos, K.; Stathopoulos, N.; Louka, P.; Tsanakas, K.; Tsesmelis, D.E.; Krassanakis, V.; Petropoulos, G.P.; Pappas, V.; Chalkias, C. Geoinformation Technologies in Support of Environmental Hazards Monitoring under Climate Change: An Extensive Review. *IJGI* **2021**, *10*, 94. [[CrossRef](#)]
30. Pradhan, B. Flood Susceptible Mapping and Risk Area Delineation Using Logistic Regression, GIS and Remote Sensing. *J. Spat. Hydrol.* **2009**, *9*, 1–18.
31. Ranaee, E.; Shoushtari, M.M.; Quchani, S.R. The Combination of HEC-Geo-HMS, HEC-HMS and MIKE11 Software Utilize in a Two Branches River Flood Routing Modeling. In Proceedings of the 2009 Second International Conference on Environmental and Computer Science, Dubai, United Arab Emirates, 28–30 December 2009; pp. 317–321.
32. Chen, J.; Hill, A.A.; Urbano, L.D. A GIS-Based Model for Urban Flood Inundation. *J. Hydrol.* **2009**, *373*, 184–192. [[CrossRef](#)]
33. Du, J.; Xie, H.; Hu, Y.; Xu, Y.; Xu, C.-Y. Development and Testing of a New Storm Runoff Routing Approach Based on Time Variant Spatially Distributed Travel Time Method. *J. Hydrol.* **2009**, *369*, 44–54. [[CrossRef](#)]
34. Chow, V.T.; Maidment, D.R.; Mays, L.W. *Applied Hydrology*; McGraw-Hill Series in Water Resources and Environmental Engineering; McGraw-Hill: New York, NY, USA, 1988; ISBN 978-0-07-010810-3.
35. Hornberger, G.M. (Ed.) *Elements of Physical Hydrology*, 2nd ed.; Johns Hopkins University Press: Baltimore, MD, USA, 2014; ISBN 978-1-4214-1373-0.

36. Guerriero, L.; Ruzza, G.; Guadagno, F.M.; Revellino, P. Flood Hazard Mapping Incorporating Multiple Probability Models. *J. Hydrol.* **2020**, *587*, 125020. [[CrossRef](#)]
37. Tufano, R.; Guerriero, L.; Annibali Corona, M.; Cianflone, G.; Di Martire, D.; Ietto, F.; Novellino, A.; Rispoli, C.; Zito, C.; Calcaterra, D. Multiscenario Flood Hazard Assessment Using Probabilistic Runoff Hydrograph Estimation and 2D Hydrodynamic Modelling. *Nat. Hazards* **2022**. [[CrossRef](#)]
38. Nuswantoro, R.; Diermanse, F.; Molkenthin, F. Probabilistic Flood Hazard Maps for Jakarta Derived from a Stochastic Rain-Storm Generator: Probabilistic Flood Hazard Maps for Jakarta. *J. Flood Risk Manag.* **2016**, *9*, 105–124. [[CrossRef](#)]
39. Nedvedova, K. Flood Protection in Historical Towns. In *WIT Transactions on the Built Environment*; Brebbia, C.A., Ed.; WIT Press: Southampton, UK, 2015; Volume 1, pp. 757–762. ISBN 978-1-78466-157-1.
40. Stathopoulos, N.; Kalogeropoulos, K.; Zoka, M.; Louka, P.; Tsesmelis, D.E.; Tsatsaris, A. An Integrated Approach for a Flood Impact Assessment on Land Uses/Cover Based on SAR Images & Spatial Analytics. The Case of an Extreme Event in Sperchios River Basin, Greece. In *GeoInformatics for Geosciences Advanced Geospatial Analysis Using RS, GIS & Soft Computing*; Stathopoulos, N., Tsatsaris, A., Kalogeropoulos, K., Eds.; Earth Observation; Elsevier: Amsterdam, The Netherlands, 2023; ISBN 978-0-323-98983-1. (In press)
41. Despiniadou, V.; Athanasopoulou, E. Flood Prevention and Sustainable Spatial Planning. The Case of the River Diakoniaris in Patras Authors: D. Vespiniadou, E. Athanasopoulou. In Proceedings of the 46th Congress of the European Regional Science Association: “Enlargement, Southern Europe and the Mediterranean”, Volos, Greece, 30 August–3 September 2006.
42. Drdácý, M.F. Impact of Floods on Heritage Structures. *J. Perform. Constr. Facil.* **2010**, *24*, 430–431. [[CrossRef](#)]
43. Karymbalis, E.; Katsafados, P.; Kalogeropoulos, K.; Karalis, S.; Chalkias, C. Flood risk assessment in small torrential catchments. In *The Geography of the Coastal and Insular Area*; Papadopoulos, A.G., Karymbalis, E., Chalkias, C., Eds.; Stamoulis: Athens, Greece, 2013; p. 340. ISBN 978-960-351-927-0.
44. Mentzafou, A.; Dimitriou, E. Hydrological Modeling for Flood Adaptation under Climate Change: The Case of the Ancient Messene Archaeological Site in Greece. *Hydrology* **2022**, *9*, 19. [[CrossRef](#)]
45. Lanza, S.G. Flood Hazard Threat on Cultural Heritage in the Town of Genoa (Italy). *J. Cult. Herit.* **2003**, *4*, 159–167. [[CrossRef](#)]
46. Wang, J.-J. Flood Risk Maps to Cultural Heritage: Measures and Process. *J. Cult. Herit.* **2015**, *16*, 210–220. [[CrossRef](#)]
47. Deschaux, J. Flood-Related Impacts on Cultural Heritage. In *Floods*; Elsevier: Amsterdam, The Netherlands, 2017; pp. 53–72. ISBN 978-1-78548-268-7.
48. Woodard, R.D. (Ed.) *The Cambridge Companion to Greek Mythology*; Cambridge University Press: Cambridge, UK; New York, NY, USA, 2007; ISBN 978-0-521-84520-5.
49. Köppen, W. Versuch Einer Klassifikation Der Klimate, Vorzugsweise Nach Ihren Beziehungen Zur Pflanzenwelt. *Geogr. Z.* **1900**, *6*, 657–679.
50. Köppen, W.; Köppen, R. *Handbuch der Klimatologie*; Gebrueder Borntraeger: Stuttgart, Germany, 1930.
51. Angelakis, A.N.; Antoniou, G.; Voudouris, K.; Kazakis, N.; Dalezios, N.; Dercas, N. History of Floods in Greece: Causes and Measures for Protection. *Nat. Hazards* **2020**, *101*, 833–852. [[CrossRef](#)]
52. Diakakis, M.; Deligiannakis, G.; Mavroulis, S. Flooding in Peloponnese, Greece: A Contribution to Flood Hazard Assessment. In *Advances in the Research of Aquatic Environment*; Lambrakis, N., Stourmaras, G., Katsanou, K., Eds.; Springer: Berlin/Heidelberg, Germany, 2011; pp. 199–206. ISBN 978-3-642-19901-1.
53. Strahler, A. Quantitative Analysis of Watershed Geomorphology. *Am. Geophys. Union Trans.* **1957**, *38*, 913–920. [[CrossRef](#)]
54. Garbrecht, J.; Shen, H.W. The Physical Framework of the Dependence between Channel Flow Hydrographs and Drainage Network Morphometry. *Hydrol. Process.* **1988**, *2*, 337–355. [[CrossRef](#)]
55. Tsanakas, K.; Karymbalis, E.; Gaki-Papanastassiou, K.; Maroukian, H. Geomorphology of the Pieria Mtns, Northern Greece. *J. Maps* **2019**, *15*, 499–508. [[CrossRef](#)]
56. Fountoulis, I.; Mavroulis, S. Flood Hazard Assessment in the Kladeos River Basin (Olympia—Western Peloponnese, Greece). In Proceedings of the AQUA 2008 3rd International Conference, Athens, Greece, 16–19 October 2008.

Disclaimer/Publisher’s Note: The statements, opinions and data contained in all publications are solely those of the individual author(s) and contributor(s) and not of MDPI and/or the editor(s). MDPI and/or the editor(s) disclaim responsibility for any injury to people or property resulting from any ideas, methods, instructions or products referred to in the content.